

## Effect of Aging under Strain on the Physical Properties of Polyester-Urethane Elastomer

Y. W. DENG,\* T. L. YU,\*† and C. H. HO\*\*

\* *Department of Chemical Engineering, Yuan-Ze Institute of Technology, Nei-Li, Taoyuan, Taiwan 32026*

\*\* *Department of Chemical Engineering, Lung Hwa Junior College of Engineering, Kwei-Shan, Taoyuan, Taiwan 33327*

(Received June 1, 1994)

**ABSTRACT:** The mechanical, degradation, and related thermal properties of segmented polyester-urethane elastomers which were aged under strain in three different environments (25°C in air, 85°C in air, and 85°C in water) were investigated by stress-strain measurements, DSC, and FTIR. From the stress-strain measurements, it showed that the polyester-urethane samples aged under a high prestrain, particularly at high temperature, resulted in decreases of the initial slope, and stress and elongation at break. The behavior of stress-strain curves also showed that aging the polyester-urethane at a higher prestrain and a higher temperature led the urethane elastomer to be more brittle. Morphological changes which were induced in the segmented elastomer by aging under strain were investigated by DSC in terms of the glass transition temperature of the soft segments, the melting temperature of the hard segments, and the heat of fusion of the crystalline hard segments. FTIR measurements indicated the degradation of the ester C—O—C bond during aging at high strain, especially in the water. Based on the DSC and FTIR studies, the behavior of the stress-strain measurements of the aged urethane elastomers was explained.

**KEY WORDS** Polyurethane / DSC / FTIR / Stress-Strain / Aging /

The segmented polyester-based urethanes are thermoplastic elastomers with high elongation characteristics, along with typical properties of plastics such as modulus, strength, and processibility. It is generally agreed that the unique mechanical properties of polyurethanes, as compared to other types of elastomers, are predominantly the result of a two-phase morphology.<sup>1,2</sup> The polyester based urethanes consist of an aromatic diisocyanate with a glycol chain extender as the hard segment and a low molecular weight aliphatic polyesters as the soft segment. They are considered to be linear segmented block copolymer, made up of alternating hard and soft block segments. Compositional variables and processing conditions are known to affect the

degree of phase segregation, phase mixing, hard segment domain organization, and subsequent polyurethane properties.<sup>2-4</sup> Depending on the relative incompatibility of the hard and soft segments, phase segregation will occur during processing and postcure annealing. The effects of polyurethane composition and structure on the resultant properties has been investigated by several researchers.<sup>5-20</sup> These studies have been concentrated on model compounds based on aromatic diisocyanates, such as toluene diisocyanate (TDI)<sup>5-6</sup> or diphenyl methane diisocyanate (MDI).<sup>5-8</sup> The phase segregation of hard and soft segment domains have been demonstrated by: small and wide angle X-ray scattering,<sup>9-12</sup> differential scanning calorimetry,<sup>9-16</sup> infrared spectroscopy,<sup>16-18</sup> and mi-

† To whom all correspondence should be addressed.

crosscopy.<sup>19-20</sup>

Various methods have been used to study hydrolytic exposure of urethane elastomers in an unstressed state. Several researchers immersed the elastomers in water at temperatures between 50–100°C.<sup>22-25</sup> Other workers investigated the urethane elastomers above water at 70–100% relative humidity and at the same temperature range.<sup>22-24</sup> One of the most comprehensive studies were conducted by Athey<sup>21</sup> on thermoplastic elastomers. The experimental results indicated that the polyether-based urethanes are less easily hydrolyzed than the polyester-based urethanes.

The effect of stress on the morphology of urethane elastomers has been reported by several workers. Based on small angle X-ray scattering data, Desper<sup>26</sup> deduced the breakup of the hard segment phase into smaller domains and associated this process in part to the manifestation of mechanical hysteresis. Infrared dichroism experiments<sup>27-29</sup> have shown that segmented polyurethane undergo some degree of irreversible orientation, especially of the hard segments, at large strains. X-ray studies<sup>30,31</sup> have confirmed the process of strain induced orientation and crystallization in polyurethanes. For many of these materials strain-induced crystallization of the soft segment matrix could be largely irreversible<sup>32-34</sup> and lead to permanent deformation and a noticeable hysteresis effect. Once crystallization has occurred, the polymer matrix might become brittle. Subsequent energy placed into the system leads to the disruption of the crystallinity inside the soft segment,<sup>32</sup> and causes crazing, bond breaking, and eventually, the failure of the polymer as a tensile break. Wang<sup>32</sup> and others<sup>33-35</sup> have shown that, for polyether polyurethane elastomers, both the hard segment and soft segment contents are key to determining the material's mechanical hysteresis response.

In this work, the physical aging of polyurethane elastomer was proceeded in three different environments (25°C in air, 85°C in

air, 85°C in water) for two days under various strain states. Stress-strain as well as DSC and FTIR measurements of these aged samples were conducted to study the effect of strain in these environments on the mechanical properties and morphology of polyester based urethane elastomers. Attempt has been made to correlate the stress-strain behavior and the morphological changes induced upon stretching of the materials.

## EXPERIMENTAL

### Materials

Poly(tetramethylene adipate) glycol (PTAd) was synthesized from butanediol and adipic acid with an OH/COOH ratio of 1.3/1.0. Thus, the polyesters had an acid number of 3 mg KOH per g, and the molecular weight  $M_n$  of the polyester determined by GPC (Waters model 746 GPC with  $\mu$ -styragel columns of pore sizes 500<sup>0</sup> Å, 10<sup>3</sup> Å, and 10<sup>4</sup> Å, and a RI detector) was found to be 2010 with a dispersion of  $M_w/M_n = 1.80$  at 25°C. Tetrahydrofuran (THF) was used as the mobile phase, and narrow MWD polystyrene standards (Aldrich Chemical Co.) were used in a linear calibration. The polyurethane elastomers were synthesized randomly from PTAd, diphenylmethane-4,4'-diisocyanate (MDI), and 1,4-butanediol (BDO) with a molar ratio of 1.5/7.1/5.5 in the *N,N*-dimethyl formamide (DMF) solvent. The reaction proceeded at 85°C for about 1 h. Before polymerization, PTAd, BDO, and DMF were distilled at 70°C under vacuum for 1 h to remove moisture. MDI was used as it received without further purification. The final polyurethane contained 57 wt% of PTAd. In order to identify the DSC thermal transition and endotherms of the soft and hard segments of aged polyurethanes, the high molecular weight pure soft segment PTAd ( $M_n = 1.8 \times 10^4$ , and  $M_w/M_n = 2.1$ ) and pure hard segment polymer were synthesized. The high molecular weight PTAd was synthesized from butanediol and adipic acid with an OH/COOH mole ratio

of 1.05/1, and the pure hard segment polymer was synthesized from BDO and MDI with a OH/NCO ratio of 1/1.

### Sample Preparation

Polyurethane films were compression-molded at 180°C on a press (Tien Fa Co., Taiwan, R.O.C.) followed by cooling at an ambient temperature and environment. Test specimens were cut in the shape of a dumbbell (ASTM D1708-66). These specimens were first elongated to each of the four designated stretching ratios (0.0%, 20%, 200%, and 400%) using an Instron Tensile Tester with a strain rate of 5.0 cm min<sup>-1</sup>. The specimens were kept stretched and were aged in each of the three environments: (1) 25°C in air for 2 days; (2) 85°C in air for 2 days; (3) 85°C in water for 2 days. After the scheduled time, specimens were unloaded and removed from the environment. All the specimens were then equilibrated to the ambient conditions before testing. The residual strains for samples with various prestrains and aged under three different environments are shown in Table I.

Film for infrared analysis were cast directly onto a NaCl plate from dilute polymer solutions (0.4 mg ml<sup>-1</sup>), prepared by dissolving the treated samples in DMF solvent, and dried

under vacuum to remove the solvent completely.

Samples cut from treated polyurethane elastomers with a weight range of 6.0–10.0 mg were used for DSC scan studies.

### Mechanical Experiment

Stress-strain curves of aged polyurethane samples were accomplished on an Instron Universal Materials Testing Machine at 25°C. The samples were subjected to a deformation rate of 5.0 cm min<sup>-1</sup> for the tension experiments. The load cell used was first calibrated, and it was found that the load remained constant within the range of experimental error. Typically, each analysis was carried out on a minimum of five samples and the average values were reported.

### Infrared Analysis

A Fourier Transform IR Spectrophotometer (Perkin Elmer 1725X) was used in this investigation. All the spectra were taken at room temperature. Subtraction of IR spectra was done using a reference peak at 1410 cm<sup>-1</sup> band, due to thermally stable C–C stretching mode of the benzene ring.

### DSC Study

Differential scanning calorimetry was carried out on a Du Pont 910 DSC. The heating rate was 20°C min<sup>-1</sup> for the temperature range –100–240°C.

## RESULTS AND DISCUSSION

### Stress-Strain Measurements

The morphology of phase segregation of these urethane elastomers is the key determining their stress-strain behavior.<sup>1,2</sup> Test specimens were subjected to a series of strains under different environments (25°C in air, 85°C in air, and 85°C in water) for two days. Typical stress-strain curves of the aged urethane samples with 0% prestrain at 25°C in air, 20% prestrain at 85°C in air, and 200% prestrain

**Table I.** Residual strain of PU aged in various environments

Prestrain	Residual strain
%	%
25°C/air/1 days	
20	3.9
200	56.5
400	115.3
85°C/air/2 days	
20	12.1
200	148.7
400	302.3
85°C/water/2 days	
20	12.8
200	161.5
400	307.7

at 85°C in water are shown in Figure 1. The stress-strain curves for polyurethane, after having been prestrained to 400% elongation, and aged in three environments (25°C in air, 85°C in air, and 85°C in water) for 2 days, are shown in Figure 2. Prior to obtaining those stress-strain curves, the prestrained samples were relaxed in air and dried. The effects of 2 days of aging in water and air with various prestrains (0%, 20%, 200%, and 400%) on the

stress-strain properties of the urethane elastomers are summarized in Table II.

It is noted that for samples aged at low prestrains (0% and 20%) the stress-strain behaviors (Figure 1 and Table II) in the three different environments were very similar. The stress-strain curves for polyurethane samples aged under low prestrains (0% and 20%) can be divided into three distinct regions. The high Young's modulus in region I (0–20% strain)

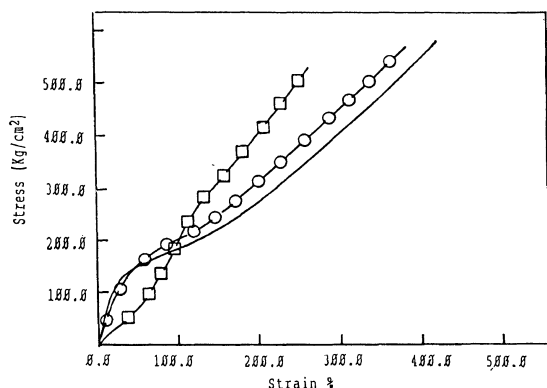


**Figure 1.** Stress-strain curves of aged polyurethanes. (—) Aged under 0% prestrain at 25°C in air; (—○—○—) aged used 20% prestrain at 85°C in air; (—□—□—) aged under 200% prestrain at 85°C in water.

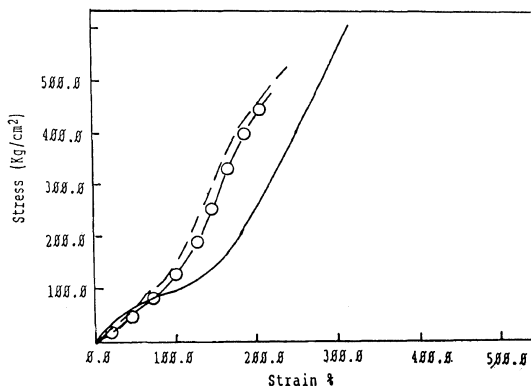


**Figure 2.** Stress-strain curves for polyurethane aged under 400% prestrain and in three different environments. (—) Aged 25°C in air; (---) aged at 85°C in air; aged at (—○—○—) 85°C in water.

**Table II.** Mechanical properties of PU aged in various environments

Prestrain	Tensile stress at 20% strain	Tensile stress at 100% strain	Tensile stress at 200% strain	Tensile stress at break	Elongation at break	Initial Young's modulus
%	kg cm <sup>-2</sup>	kg cm <sup>-2</sup>	kg cm <sup>-2</sup>	kg cm <sup>-2</sup>	%	kg cm <sup>-2</sup>
25°C/air/2 days						
0	110.4	187.6	287.0	583.0	430	758.5
20	99.4	187.7	292.5	589.0	410	625.5
200	52.4	157.3	328.4	593.0	350	320.6
400	33.1	99.4	231.8	614.0	315	180.0
85°C/air/2 days						
0	91.1	182.1	276.0	575.0	425	551.3
20	88.3	198.7	314.6	574.0	395	500.4
200	35.9	253.9	436.0	560.0	265	187.7
400	27.6	156.1	447.0	523.0	250	146.6
85°C/water/2 days						
0	102.1	184.0	281.5	573.0	425	586.5
20	74.5	193.2	314.6	558.0	390	412.4
200	27.6	215.3	405.7	528.0	260	164.2
400	22.1	124.2	430.5	479.0	220	125.1

is due to the elastic deformation of the soft segment domain. At higher elongations, in region II (20–200% strain), rupturing of the hydrogen bonding of the short range hard segments occurred. This event may then lead to molecular slippage, chain disentanglement, and phase mixing. As the elongation increased, the soft segment molecules moved from transverse to parallel to the draw direction which induced crystallization. By completing the crystallite orientation, the polymer matrix becomes brittle and the stress again rises rapidly with increasing elongation (>200% strain, region III). Comparing the stress–strain curves of samples aged under 20% prestrain with those aged without prestrain, the stress was slightly higher in the case of strain being higher than 100% for samples aged under 20% prestrain than those aged without prestrain. This phenomenon could be due to the crystallization of soft segments aged under 20% prestrain.

However, for samples aged under highly prestrain (200% and 400% prestrain), the stress–strain curves (Figures 1 and 2 and Table II) were quite different from those aged under low prestrain (0% and 20%) as shown by the stress–strain data (Table II). The data indicated that the samples aged under a higher prestrain had a lower initial slope (Young's modulus) and a lower elongation at break. For the samples aged under a low prestrain, the stress–strain curves of different aging environments were very similar; while the shape of the stress–strain curves for samples aged under a high prestrain strongly depended upon the aging temperature and environment. Aging under a high prestrain, when the aging temperature was increased, the samples had higher stress in the high strain region (strain higher than 70%) and lower stress was found in the low strain region of the stress–strain data (Table II). Comparing the stress–strain data of polyurethane elastomers aged at 85°C in air and 85°C in water, we also found that the stress was lower over whole range of strain for samples aged at 85°C in water.

For samples aged in the same environments but with various prestrains, the stress–strain data showed an increase in brittleness as aging prestrain was increased. This phenomenon may be due to the fact that at higher prestrain complete orientation of the hard segments parallel to the draw direction caused an increase in the degree of crystallinity of the hard segments and brittleness (as shown by the DSC data in the following sections). From Table II, we also noticed that the stress at break increased with increasing prestrain for samples aged at room temperature. However, the stress at break decreased with increasing prestrain for samples aged at higher temperatures. The samples aged at a high temperature also exhibited a lowering Young's modulus with increasing aging prestrain. The behaviors of lower Young's modulus and stress at break of stress–strain measurement for urethanes aged under a high prestrain and high temperature may be due to the chain scission of the ester linkage in the soft segments (as shown by the FTIR data in the following sections).

In the following sections, DSC data demonstrated the variations of morphology of polyurethanes aged under various conditions and FTIR results showed the evidence of the degradation of polyester C–O–C bonds for urethanes aged under a high prestrain and at higher temperature.

#### *DSC Analysis*

The DSC curves of pure soft segment polymer (high molecular weight PTAd) and pure hard segment (copolymers of BDO and MDI) which were aged without prestrain at 25°C in air are shown in Figure 3. The positions of the DSC endotherms and thermal transitions are listed in Table III. As indicated in Figure 3 and Table III, the glass transition temperature ( $T_{g1}$ ) and melting endothermal ( $T_{m1}$ ) were around  $-51^{\circ}\text{C}$  and  $48^{\circ}\text{C}$  respectively. The small endotherm due to short range order hydrogen bonding ( $I_2$ )<sup>36</sup> and the melting endotherm of microcrystalline domain ( $T_{m2}$ )

were around 66°C and 170–220°C respectively.

Typical DSC curves of the aged urethane samples under various prestrains are shown in Figure 4 for the aging conditions of 25°C in air with 200% and 400% prestrain, 85°C in air with 0% prestrain, and 85°C in water with 20%

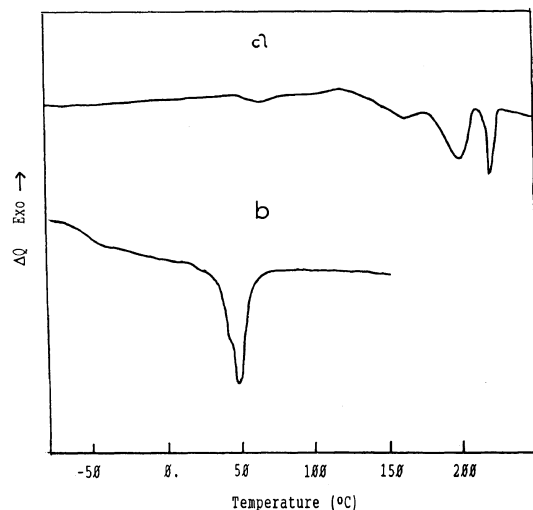


**Figure 3.** DSC curves of (a) pure hard segment (copolymer of BDO and MDI); (b) pure PTAd ( $M_n = 1.8 \times 10^4$  and  $M_w/M_n = 2.1$ ).

prestrain. The samples were strained for two days prior to the DSC experiments. Table III lists the position of the DSC endotherms and the thermal transitions of the prestrained samples aged under various environments. The uncertainty associated with each temperature

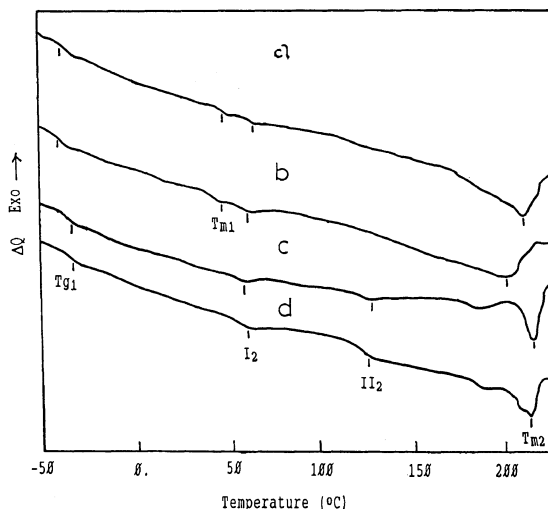


**Figure 4.** DSC curves of polyurethanes aged under: (a) 200% prestrain at 25°C in air; (b) 400% prestrain at 25°C in air; (c) 0% prestrain at 85°C in air; and (d) 20% prestrain at 85°C in water.

**Table III.** Thermal properties of aged polyurethanes

Prestrain	$T_{g1}/^{\circ}\text{C}$	$T_{m1}/^{\circ}\text{C}$	$I_2/^{\circ}\text{C}$	$II_2/^{\circ}\text{C}$	$T_{m2}/^{\circ}\text{C}$	$\Delta H_f/\text{cal g}^{-1}$
PU/25°C/air/2 days						
0%	-33	—	65	—	210	8.09
20%	-36	—	63	—	210	8.79
200%	-37	45	65	—	211	9.66
400%	-39	46	62	—	203	11.07
PU/85°C/air/2 days						
0%	-32	—	57	125	214	7.80
20%	-33	—	58	123	210	8.95
200%	-33	—	—	—	209	9.60
400%	-34	—	—	—	210	10.84
PU/85°C/water/2 days						
0%	-30	—	60	125	210	7.66
20%	-32	—	60	124	211	8.94
200%	-33	—	—	—	210	9.24
400%	-33	—	—	—	202	10.60
PTAd ( $M_n = 1.8 \times 10^4$ )/25°C/air/2 days						
0%	-51	48	—	—	—	—
Pure Hard Segment/25°C/air/2 day	—	—	66	—	198 and 217	—

is approximately  $\pm 2^\circ\text{C}$ .

The prestrained urethane samples, aged under ambient conditions ( $25^\circ\text{C}$  in air) generally exhibited three transition regions detected by DSC as shown in Figure 4 and Table III. Between  $-30^\circ\text{C}$  and  $-40^\circ\text{C}$ , a sharp increase in the specific heat occurs, and is due to the soft-segment glass transition ( $T_{g1}$ ). The  $T_g$  of the soft segment domains, is an indicator for the degree of phase separation. When there were hard segments dispersed in the soft domains, the  $T_{g1}$  was raised. It is found that  $T_{g1}$  shifts slightly to lower temperatures when the samples were subjected to higher prestrains (Table III). This implies that prestrain would promote phase demixing of hard and soft segments favoring pure soft domains. Between  $60^\circ\text{C}$  and  $65^\circ\text{C}$  a small endotherm occurs ( $I_2$ ), due to the dissociation of short range ordering in the hard segment domain.<sup>32,36</sup> For samples aged at  $25^\circ\text{C}$  and under a high prestrain ( $\geq 200\%$  elongation), a small endotherm appeared around  $45^\circ\text{C}$ , due to the melting endotherm ( $T_{m1}$ ) of the soft segment crystallization induced by strain. The primary endotherm ( $T_{m2}$ ) was found in the third region ( $170$ – $230^\circ\text{C}$ ) with the multiple peaks, which could be the sequential melting/distruption of hard-segment domains having different degrees of organization.<sup>36</sup> This endotherm was not affected by prestrain in this study, however, the heat of fusion,  $\Delta H_f$ , increased with increasing prestrain during aging. Crystallization requires an exact arrangement of hard segments into a lattice structure and thus has a well defined temperature associated with melting. Therefore, the present data indicated that prestrain may be expected to change the shape or size of the crystalline melting peak, but not its position unless significant changes are made in crystallite size or perfection. The crystallite size increased with increasing prestrain. These different degrees of organization were developed depending upon prior thermal and processing history of the elastomers. It is noted that when the aging prestrain reached  $400\%$ ,

the multiple melting peaks disappeared and turned into a broad endotherm.

Similar behavior of the glass transition temperature ( $T_{g1}$ ) of the soft segment, melting temperature ( $T_{m2}$ ) of the microcrystalline domain, and endotherm of hard segment ( $\Delta H_f$ ) for the sample aged at  $85^\circ\text{C}$  in air as those aged at  $25^\circ\text{C}$  in air were found. (Table III and Figure 4). The  $T_{g1}$  of the soft segment slightly decreased and the heat of fusion,  $\Delta H_f$ , of microcrystalline domain increased as the prestrain increased during aging. In contrast to the prestrained samples aged at  $25^\circ\text{C}$ , the  $T_{g1}$  of the soft segments was increased by aging the samples at a higher temperature, indicating that annealing at high temperature could promote mixing of soft and hard domains and result in a higher  $T_{g1}$ . The heat of fusion,  $\Delta H_f$ , of microcrystalline decreased as the aging temperature increased, suggesting the rupture of hydrogen bond in the microcrystalline domain at high temperature. Comparing to the samples aged in air at  $25^\circ\text{C}$ , the other difference in the thermal behavior of samples aged at  $85^\circ\text{C}$  in air, was the appearance of an endotherm ( $II_2$ ) in the  $110$ – $130^\circ\text{C}$  range for urethane samples with low prestrains ( $0\%$  and  $20\%$ ). This endotherm might be due to the dissociation of long-range ordering hard-segment domains.<sup>36</sup> For aging at  $85^\circ\text{C}$  with prestrain higher than  $200\%$ , the endotherms of short range ordered hard segment domain ( $I_2$ ) and long range ordered hard segment domain ( $II_2$ ) disappeared, and the shape of the crystalline hard segment domain ( $T_{m2}$ ) were broader than those aged under lower prestrain. These data suggested that aging under high prestrain and high temperature resulted in an increase of the size of the crystalline hard domain.

The DSC data of the prestrained samples aged at  $85^\circ\text{C}$  under water were similar to those of samples aged at  $85^\circ\text{C}$  in air in the following patterns: the appearance of  $I_1$  and  $II_2$  endotherms at lower prestrains; and the disappearance of  $I_1$  and  $I_2$  endotherms and the

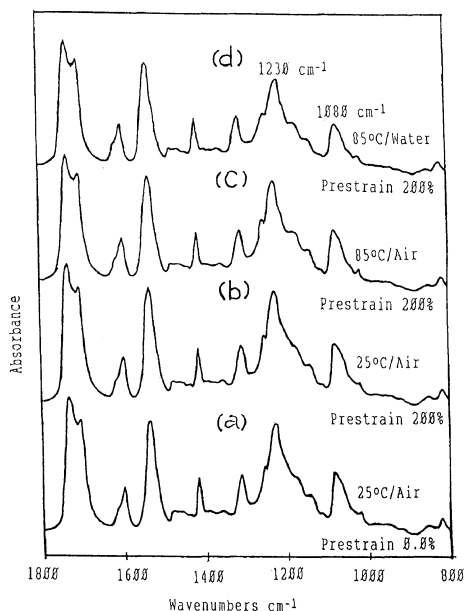


**Figure 5.** FTIR spectra of polyurethane aged in four different conditions. (a) 0% prestrain, 25°C in air; (b) 200% prestrain, 25°C in air; (c) 200% prestrain, 85°C in air; (d) 200% prestrain, 85°C in water.

broadening of the microcrystalline domain ( $T_{m2}$ ) in the highly prestrained samples. (Table III and Figure 4).

In general,  $T_{g1}$  decreased with increasing aging prestrain and increased with increasing aging temperature; while  $T_{m2}$  remained constant with increasing prestrain and aging temperature and seems not to depend on the environment that the samples were subjected to. The heat of fusion,  $\Delta H_f$ , increased with increasing prestrain and decreased with increasing aging temperature.

#### Infrared Analysis

As shown in the previous section, the stress-strain data for urethanes aged under a high prestrain strongly depended upon the aging temperature and environment. Hence, the urethane samples aged under 200% prestrain in three different environments were investigated by FTIR. The IR spectra of 200% prestrained polyesterurethane samples aged in three environments (25°C in air, 85°C in air

**Table IV.** Absorbance of ester and urethane C–O–C stretching for PU aged at various conditions

Aging condition	1250–1180	1100–1030
	cm <sup>-1</sup>	cm <sup>-1</sup>
25°C/air/ 0% prestrain	87.2	91.4
25°C/air/200% prestrain	87.0	91.2
85°C/air/200% prestrain	84.6	89.1
85°C/water/200% prestrain	83.3	87.1

Note: The absorbance are given using the 1430–1400 cm<sup>-1</sup> band equals 10 as a reference.

and 85°C in water) are presented in Figure 5. According to the IR spectra absorption band assignment by Silverstein *et al.*,<sup>37</sup> the very strong band that occurs at 1230 cm<sup>-1</sup> is considered to be the ester C–O–C unsymmetric stretching of the ester and urethane groups mixed with CH<sub>2</sub> wagging mode. Another band appearing at 1080 cm<sup>-1</sup> is attributed to ester C–O–C symmetric stretching of the ester and urethane groups. Table IV shows the changes of the intergrated absorption peak area ( $A$ ) of the C–O–C stretching of the 200% prestrained samples aged in air and water at various temperatures, using the 1410 cm<sup>-1</sup> band, which is a thermally stable C–C stretching in the benzene ring as a reference peak. The water-aged samples were found to be more degraded than the air-aged samples, especially at higher temperature.

#### CONCLUSION

Very similar stress–strain curves of urethane elastomers aged under low presstrains (0% and 20%) in three environments (25°C in air, 85°C in air, and 85°C in water) were obtained. However, for urethane elastomers aged under high prestrains (200% and 400%), the behavior of stress–strain curves was strongly influenced by the aging environments. Aging at a high prestrain, with increasing aging temperature caused a decrease in the initial slope of stress–



strain measurement, and an increase in brittleness of urethanes. Aging at a high temperature also resulted in decreases both in tensile stress and elongation at break. Comparing samples aged at a high temperature but under various prestrains, we found that aging at a higher prestrain resulted in lowering the initial slope of stress-strain curve, stress at break, and elongation at break. FTIR experimental data revealed the degradation of ester C—O—C bond for polyurethane elastomers aged at a high temperature with a high prestrain, especially under water which may be the reason for the lowering of the initial slope of the stress-strain curve and the tensile stress at break and elongation at break. DSC experimental results demonstrated the increase in microcrystalline domain induced by increasing prestrain during aging. The crystallization of urethane elastomers induced by prestrain during aging leads to the behavior of brittleness. The FTIR experimental results also revealed that more degradation of ester C—O—C bond for urethane elastomers aged under water than aged in air which caused the behavior of lower stress over the whole range of strain of stress-strain curves for urethane elastomers aged under water at 85°C than under air at 85°C.

## REFERENCES

- S. L. Copper and A. V. Tobolsky, *J. Appl. Polym. Sci.*, **10**, 1837 (1966).
- T. K. Kwei, *J. Appl. Polym. Sci.*, **27**, 2891 (1982).
- D. S. Huh and S. C. Cooper, *Polym. Eng. Sci.*, **11**, 369 (1971).
- C. E. Wilkes and C. S. Yusek, *J. Macromol. Sci. Phys.*, **B7**, 157 (1973).
- (a) G. G. Seefried, Jr., J. V. Koleske, and F. E. Critchfield, *J. Appl. Polym. Sci.*, **19**, 2493 (1975); (b) *ibid.*, 3185.
- G. W. Miller and J. H. Saunders, *J. Polym. Sci.*, **A-18**, 1923 (1970).
- S. Abouzahr and G. L. Wilkes, *J. Appl. Polym. Sci.*, **29**, 2695 (1984).
- J. A. Miller, S. B. Lin, K. K. S. Hwang, K. S. Wu, P. E. Gibson, and S. L. Cooper, *Macromolecules*, **18**, 32 (1985).
- R. W. Seymour and S. L. Cooper, *Macromolecules*, **6**, 48 (1973).
- J. T. Koberstein and A. F. Galambos, *Macromolecules*, **25**, 5618 (1992).
- J. T. Koberstein, A. F. Galambos, and L. M. Leung, *Macromolecules*, **25**, 6195 (1992).
- J. T. Koberstein and L. M. Leung, *Macromolecules*, **25**, 6205 (1992).
- C. S. Paik Sung, C. B. Hu, and C. S. Wu, *Macromolecules*, **13**, 111 (1980).
- J. A. Miller and S. L. Copper, *J. Polym. Sci., Polym. Phys. Ed.*, **23**, 1065 (1985).
- L. M. Leung and J. T. Koberstein, *Macromolecules*, **19**, 706 (1986).
- J. T. Koberstein and I. Gancarz, *J. Polym. Sci., Polym. Phys. Ed.*, **24**, 2487 (1986).
- J. C. West and S. L. Cooper, *J. Polym. Sci., Polym. Symp.*, **60**, 27 (1977).
- M. M. Coleman, K. H. Lee, D. J. Skrovanek, and D. C. Painter, *Macromolecules*, **19**, 2149 (1986).
- G. L. Wilkes, S. L. Samuel, and R. G. Crystal, *J. Macromol. Sci.-Phys.*, **B10**, 203 (1974).
- J. Foka and H. Janik, *Polym. Eng. Sci.*, **29**, 113 (1989).
- R. J. Athey, *Rubber Age*, **96**, 705 (1965).
- G. Magnu, R. A. Dunleavy, and F. E. Critchfield, *Rubber Chem. Tech.*, **39**, 1328 (1966).
- F. H. Gahimer and F. W. Nieske, *J. Elastoplastics*, **1**, 26 (1967).
- H. Y. Bonk and A. A. Sardanopoli, *J. Elastoplastics*, **4**, 157 (1971).
- A. Sign and R. Saxon, *Rubber Age*, **107**, 53 (1975).
- C. R. Desper, N. S. Schneider, J. P. Jasinski, and J. S. Lin, *Macromolecules*, **18**, 2755 (1985).
- R. W. Seymour, A. E. Allegrazza, and S. L. Copper, *Macromolecules*, **6**, 896 (1973).
- A. E. Allegrazza, R. W. Seymour, H. N. Ny, and S. L. Copper, *Polymer*, **15**, 433 (1974).
- G. M. Estes, R. W. Seymour, and S. L. Cooper, *Macromolecules*, **4**, 452 (1971).
- C. F. Wilkes and C. S. Yusek, *J. Macromol. Sci.-Phys.*, **B7**, 157 (1973).
- R. Bonart, *J. Macromol. Sci.-Phys.*, **B2**, 115 (1968).
- C. B. Wang and S. L. Cooper, *Macromolecules*, **16**, 775 (1983).
- C. S. P. Sung, T. W. Smith, and N. H. Sung, *Macromolecules*, **13**, 117 (1980).
- C. S. P. Sung, T. W. Smith, C. B. Hu, and N-H. Sung, *Macromolecules*, **12**, 538 (1979).
- L. L. Harrell, *Macromolecules*, **2**, 607 (1969).
- T. R. Hesketh, J. W. C. van Bogart, and S. L. Cooper, *Polym. Eng. Sci.*, **20**, 190 (1980).
- R. M. Silverstein, G. Clayton, and T. C. Morrill, in "Spectrometric Identification of Organic Compounds," 4th ed., John Wiley & Sons, New York, 1981.